

**RECENT MISSION OBSERVATIONS PROVIDE SCIENTIFIC CONTEXT AND ENABLING SUPPORT FOR FUTURE EXPLORATION OF THE MOON'S SOUTH POLE-AITKEN BASIN.** B. L. Jolliff<sup>1</sup>, N. E. Petro<sup>2</sup>, <sup>1</sup>Department of Earth & Planetary Sciences and The McDonnell Center for the Space Sciences, Washington University, One Brookings Drive, St. Louis, MO 63130, <sup>2</sup>NASA Goddard Space Flight Center, Planetary Geodynamics Laboratory. (blj@wustl.edu)

**Introduction:** The Moon's South Pole-Aitken (SPA) Basin is a scientifically rich destination for future exploration by landed and sample-return missions. The current Planetary Science Decadal Survey [1] recognized this scientific potential in terms of the SPA basin's importance for recording the chronology of major events in the early Solar System as well as for understanding lunar history, structure, and giant impact processes. Current and recent orbital mission results including LRO, GRAIL, Chandrayaan-1, and Kaguya are paving the way for an improved understanding of SPA basin geology and history, and indeed, posing new questions for future exploration.

**Topography and Geophysics:** Topography of the SPA basin has been well determined from the combined LRO LOLA (Lunar Orbiter Laser Altimeter) and LROC WAC (Wide Angle Camera) topographic data sets (Fig. 1) [e.g., 2,3]. These data enable unprecedented morphometric analysis of surface landforms as well as geologic analysis of volcanic and crater deposits [e.g., 4]. For specific locations, NAC-derived digital topographic models (DTM) of the terrain are available at meter-scale resolution. One of the key science results has been the definition of large areas of ancient, buried mare basalts (cryptomare) within the basin, which contribute to the mafic (FeO-rich) compositional character of the basin interior [4-6]. A key objective for future *in situ* exploration is to determine the origin of this mafic signature, which is likely a combination of basalt, mafic crustal rocks, or exposed mafic impact-melt cumulates (see below).

High-resolution gravity measurements from GRAIL has led to new models for crustal thickness and density [7]. For SPA basin, gravity data indicate a typical crustal thickness of ~20 km within SPA and minimum values of 5 km or less at Poincaré and Apollo basins. Additionally, the SPA basin interior has among the highest crustal densities on the Moon. These observations have been interpreted to indicate that the thick impact-melt "sea" produced by the SPA event differentiated and produced a noritic upper layer, which is mainly what has been exposed in impact-crater central peaks [8]. Samples from the interior of the basin

would help constrain models for the formation of such a large basin and the possible role of impact-melt differentiation.

Topographic data coupled with a WAC image mosaic with lighting optimized for morphology also has enabled new crater size-frequency distribution (CSFD) analyses that can be used to estimate relative ages of surfaces within SPA basin. Hiesinger et al. [9] determined CSFDs indicating an ~4.26 Ga model age for SPA and model ages between ~4.0 and 4.1 Ga for several other large craters (Planck and Oppenheimer) within SPA. These model ages have huge potential implications for the early Solar System flux of large impactors and possible causes and duration of the increased flux between 4.2 and 3.9 Ga, and reinforce the importance of returning samples from SPA basin for laboratory-based geochronology. Obtaining an absolute age for the basin from returned samples would constrain the CSFD model ages across the basin and provide improved constraints on model ages for ancient surfaces across the Solar System.

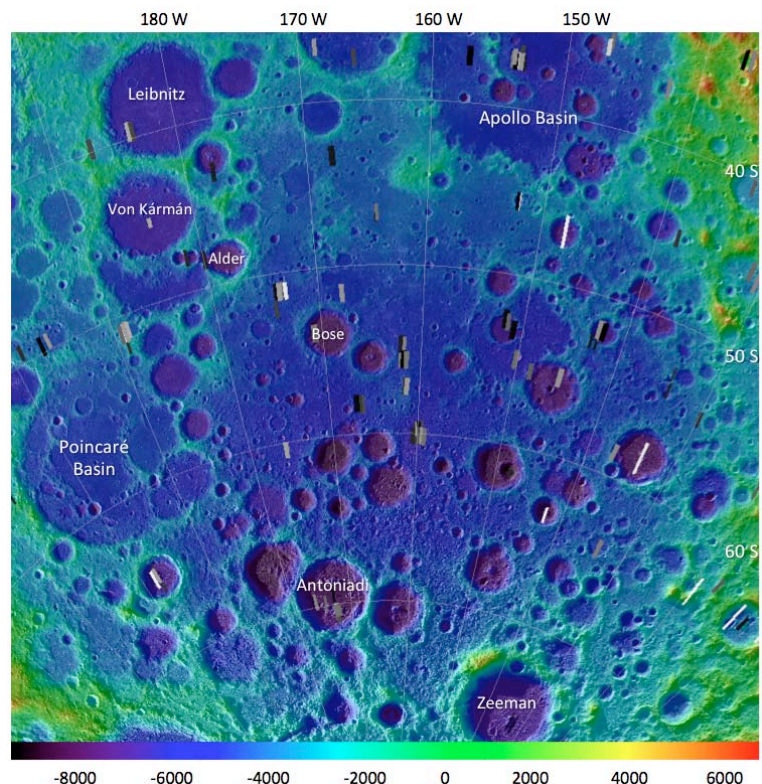


**Figure 1.** LROC WAC base mosaic overlain by GLD100 WAC-derived DTM [3] (scale in meters) showing current NAC geometric stereo image coverage.

**Geochemistry:** Several multispectral and hyperspectral data sets cover parts or all of the SPA basin, including Clementine UV-VIS, Kaguya Spectral Profiler (SP) and Multiband Imager (MI), Chandrayaan-1 Moon Mineralogy Mapper (M<sup>3</sup>), and LRO's WAC and Diviner. Clementine provided a UV-VIS spectra-based estimate of FeO abundance [10], and the Lunar Prospector gamma-ray spectrometer obtained maps of Fe, Th, and other elements [11]. Disagreement in the details of these data sets remains, but both data sets reflect the mafic character of SPA basin rocks relative to the surrounding anorthositic highlands. Multispectral and hyperspectral data also reveal mafic mineralogy, with very few anorthositic exposures [12], and the mafic component of SPA's interior appears to be dominated by low-Ca pyroxene [13,14], although pigeonite may be a significant component of the integrated pyroxene signature. Using Kaguya's SP and MI data, [15] reported a dearth of olivine-rich exposures in the interior of SPA, indicating no direct exposure of olivine-bearing mantle material and implying deep sequestration of olivine-rich rocks during SPA impact-melt differentiation.

**Landing site characterization for science and landing site safety:** In addition to use in morphometric studies, high-resolution DTMs are needed for landing-site safety assessments (i.e., slope analysis and meter-sized boulder distribution) for future landed missions. Such data have been collected for the Constellation regions of interest, including several sites within SPA Basin [16]. NAC imaging suitable for DTM generation has been obtained for about 20 sites within the basin but the total area covered is only about 0.3% (Fig. 1); additional imaging for geometric stereo is planned for the LRO second extended mission.

**Looking Forward:** The current data sets provide a superb basis for scientific landing-site selection studies. As an example, a site located near the center of the SPA basin might be located on a smooth-plains surface that is determined to be a buried mare surface (e.g., sites near Bose Crater (Fig. 1). Regolith developed on such plains would consist of a mixture of ancient volcanics, whose age and composition will reveal the Moon's early thermal and magmatic evolution in the SPA region and underlying mantle. Fragments of these volcanics along with younger volcanics have been excavated and mixed by small impacts into regolith on these surfaces. Also expected in the regolith are major proportions (>50%) of rock material excavated from the SPA impact-melt sheet itself. The numerous large craters in the 50-120 km size range and small basin-size impacts within SPA, largely excavated and ejected material derived from the SPA melt sheet. However, some small basins such as 320 km diameter Poincaré

may have excavated through such a melt sheet into the underlying lower-crust/upper mantle [17,18]. Analysis of these materials returned to Earth will reveal the components and their origins that make up the SPA basin interior with important implications for understanding the early history of the inner Solar System as well as the early evolution of the lunar crust. Results from the sample site will enable improved interpretations for all of SPA based on the remotely sensed data for the entire basin, and knowledge of actual lithologic components (ground truth) will allow unambiguous identification of SPA materials among the growing lunar meteorite collection [19,20].

**Acknowledgements:** Support for this work is primarily through LROC/ASU contract NNG07EK00C (BLJ).

**References:** [1] NRC (2011) Vision and Voyages for Planetary Science in the Decade 2013-2022. [2] Potter, R., et al. (2012) Constraining the size of the SPA basin impact, *Icarus*, **220**, 730-743. [3] Scholten, F., et al. (2012) GLD100: The near-global lunar 100 m raster DTM from LROC WAC, *J. Geophys. Res.*, **117**, E00H17. [4] Petro, N., et al. (2011) Geomorphic terrains and evidence for ancient volcanism within NE SPA., *GSA Spec. Pap.* 477. [5] Jolliff, B., et al. (2011) SPA basin interior: Topographic expression of mare, cryptomare, and nonmare plains units. *Lunar Planet. Sci.*, **42**, #2774. [6] Gibson, K., and Jolliff, B. (2011) Correlation of surface units and FeO concentrations in the SPA basin interior. *Lunar Planet. Sci.*, **42**, #2326. [7] Wieczorek, M., et al. (2013) The crust of the Moon as seen by GRAIL, *Science*, **339**, 671-675. [8] Vaughan, W., and Head, J. (2013) Impact melt differentiation in the SPA basin, *Planet. Space Sci.* [9] Hiesinger, H., et al. (2012) New crater size-frequency distribution measurements of the SPA basin, *Lunar Planet. Sci.*, **43**, #2863. [10] Lucey, P., et al. (1998) FeO and TiO<sub>2</sub> concentrations in the SPA basin: Implications for mantle composition and basin formation, *J. Geophys. Res.*, **103**, 3701-3708. [11] Lawrence, D., et al. (2003) Regional elemental abundances within SPA basin., *Lunar Planet. Sci.*, **34**, #1679, 2003. [12] Ohtake, M., et al. (2009) The global distribution of pure anorthosite on the Moon, *Nature*, **461**, 236-241. [13] Pieters, C., et al. (2001) Rock types of the SPA basin and extent of basaltic volcanism, *J. Geophys. Res.*, **106**, 28,001-28,022. [14] Moriarty, D., et al. (2013) Compositional heterogeneity of central peaks within the SPA basin, *J. Geophys. Res.*, **118**, 2310-2322. [15] Yamamoto, S., et al. (2012) Olivine-rich exposures in the SPA basin, *Icarus*, **218**, 331-344. [16] Jolliff, B., et al. (2012) LRO targeting of the SPA basin for the extended science mission. *NASA Lunar Science Forum*, July 17-19, Ames, Sunnyvale, CA. [17] Petro, N., and Pieters, C. (2004) Surviving the heavy bombardment: Ancient material at the surface of SPA basin, *J. Geophys. Res.*, **109**, E06004. [18] Petro, N., and Jolliff, B. (2013) Thin crust in the SPA basin and samples from the mantle?., *Lunar Planet. Sci.* **44**, #2724. [19] Mercer, C., et al. (2013) New lunar meteorite Northwest Africa 2996: A window into far-side lithologies and petrogenesis, *Meteorit. Planet. Sci.*, **48**, 289-315. [20] Zeigler, R., et al. (2013) Lunar meteorites Sayh al Uhaymir 449 and Dhofar 925, 960, and 961., *Lunar Planet. Sci.*, **44**, #2437.